

Lepton-Flavor-Violation in τ -Production at *BABAR* – A Search for $e^+e^- \rightarrow l^+\tau^-$

S. Schenk^{a*}

^aPhysikalisches Institut, Universität Heidelberg,
Philosophenweg 12, 69120 Heidelberg, Germany

We report on a search for the lepton-flavor-violating processes $e^+e^- \rightarrow \mu^+\tau^-$ and $e^+e^- \rightarrow e^+\tau^-$. The data sample corresponds to an integrated luminosity of 211 fb^{-1} recorded by the *BABAR* experiment at the SLAC PEP-II asymmetric-energy *B* Factory at a center-of-mass energy of $\sqrt{s} = 10.58 \text{ GeV}$. We find no evidence for a signal and set the 95% confidence level upper limits on the cross sections to be $\sigma_{\mu\tau} < 4.6 \text{ fb}$ and $\sigma_{e\tau} < 10.1 \text{ fb}$. The ratios of the cross sections with respect to the dimuon cross section are measured to be $\sigma_{\mu\tau}/\sigma_{\mu\mu} < 4.0 \times 10^{-6}$ and $\sigma_{e\tau}/\sigma_{\mu\mu} < 8.9 \times 10^{-6}$.

1. INTRODUCTION

Within the Standard Model (SM), lepton-flavor-conservation is not protected by an established gauge principle. Extensions to the SM which include our knowledge of neutrino masses and mixing [1] predict lepton-flavor-violation (LFV) in τ -decays at a level many orders of magnitude below the current experimental sensitivity ($\mathcal{B}(\tau^\pm \rightarrow \mu^\pm\gamma) \sim \mathcal{O}(10^{-54})$) [2–5].

Searches for LFV have primarily concentrated on the decay of the lepton. Limits in a number of muon decay channels have reached the 10^{-11} – 10^{-12} level [4] while recent measurements of LFV in tau decays have placed limits on the branching fractions $\mathcal{B}(\tau^\pm \rightarrow \mu^\pm\gamma) < 6.8 \times 10^{-8}$ and $\mathcal{B}(\tau^\pm \rightarrow e^\pm\gamma) < 1.1 \times 10^{-7}$ [5] at the 90% confidence level (CL).

1.1. Predictions and Experimental Status

There are theories that suggest lepton-flavor can be conserved in lepton decay but still be violated in production. Some of these models predict cross section ratios for channels such as $e^+e^- \rightarrow \mu^+\tau^-$ and $e^+e^- \rightarrow e^+\tau^-$ up to $\sigma_{l\tau}/\sigma_{\mu\mu} \sim \mathcal{O}(10^{-4})$ at center-of-mass (CM) energies $\sqrt{s} = 10.58 \text{ GeV}$ [6]. Experimental limits on

LFV in production are considerably weaker than for decay. At CM energies, $\sqrt{s} = 29 \text{ GeV}$, there are limits on the cross section ratios $\sigma_{\mu\tau}/\sigma_{\mu\mu} < 6.1 \times 10^{-3}$ and $\sigma_{e\tau}/\sigma_{\mu\mu} < 1.8 \times 10^{-3}$ (95% CL) [7]; at $\sqrt{s} = 92 \text{ GeV}$, where Z^0 exchange dominates, $\sigma_{\mu\tau}/\sigma_{\mu\mu} < 3.6 \times 10^{-4}$ and $\sigma_{e\tau}/\sigma_{\mu\mu} < 2.9 \times 10^{-4}$ (95% CL) [4,8]. The best limits from searches at LEP energies above the Z^0 peak are $\sigma_{\mu\tau}/\sigma_{\mu\mu} < 2.4 \times 10^{-2}$ and $\sigma_{e\tau}/\sigma_{\mu\mu} < 2.9 \times 10^{-2}$ (95% CL) for the energy range $\sqrt{s} = 200 - 209 \text{ GeV}$ [9]. The huge data sets accumulated by the *B* Factories *BABAR* and *BELLE* are ideally suited to achieve a new level of precision in these searches.

We present results on two modes of the process $e^+e^- \rightarrow l^+\tau^-$, where l^+ is an electron or muon and the τ^- decays either to $\pi^-\pi^+\pi^-\nu_\tau$ (3-prong) or $\pi^-\nu_\tau$ (1-prong). The analysis uses data recorded by the *BABAR* detector at the SLAC PEP-II asymmetric-energy e^+e^- storage rings. Inclusion of the charge-conjugate reaction $e^+e^- \rightarrow l^-\tau^+$ is assumed throughout this paper. The data sample corresponds to an integrated luminosity of $\mathcal{L} = 211 \text{ fb}^{-1}$ recorded at a CM energy of $\sqrt{s} = 10.58 \text{ GeV}$.

2. DETECTOR AND SIMULATION

The *BABAR* detector is described in detail in Ref. [10]. Charged particles are reconstructed as tracks with a 5-layer silicon vertex tracker

*For the *BABAR*-Collaboration. Supported by the Studienstiftung des deutschen Volkes. E-mail: schenk@physi.uni-heidelberg.de

(SVT) and a 40-layer drift chamber (DCH) inside a 1.5 T solenoidal magnet. Electrons and photons are identified using an electromagnetic calorimeter (EMC). A ring-imaging Cherenkov detector (DIRC) is used to identify charged hadrons and provides additional electron identification information. Muons are identified by an instrumented magnetic flux return (IFR).

Monte Carlo (MC) simulation is used to evaluate the background contamination and selection efficiency. The simulated backgrounds are also used to cross-check the selection optimization procedure and for studies of systematic effects; however, the final background yield estimation relies solely on data. The signal $e^+e^- \rightarrow l^+\tau^-$ channels are simulated using `EvtGen` [11] in which radiation is handled by the `PHOTOS` package [12] to an accuracy better than 1%. The background τ -pair events are simulated using the `KK2F` MC generator [13]. The τ decays are modeled with `TAUOLA` [14] according to measured rates with the decay $\tau^- \rightarrow \pi^-\pi^+\pi^-\nu_\tau$ assuming an intermediate $a_1^-(1260)$ axial-vector state [4,15]. We also generate light quark continuum events ($e^+e^- \rightarrow q\bar{q}$, $q = u, d, s$), charm, dimuon, Bhabhas, $B\bar{B}$ and two-photon events [11,16]. The detector response is simulated with `GEANT4` [17] and all simulated events are reconstructed in the same manner as data.

3. EVENT SELECTION

The signature of the signal process in the CM frame is an isolated high-momentum muon or electron recoiling against either one or three charged pions and no neutral particles. The reconstructed mass of the missing neutrino should be consistent with a massless particle and the invariant mass of the recoiling pions and neutrino consistent with that of the τ .

We search for events with zero total charge and either two or four well-measured charged tracks originating from near the e^+e^- interaction point. All charged tracks must be isolated from neutral energy deposits in the EMC and be within the acceptance of the EMC, DIRC and IFR to ensure good particle identification. One track must be identified as either an electron or muon with a

CM momentum greater than 4.68 GeV/c and no other track identified as a kaon or lepton. Events with converted photons are also rejected, where a converted photon is defined to be a pair of oppositely charged tracks assumed to have the electron mass and coming from a vertex with a combined mass of less than 150 MeV/c².

In the CM system, the event topology must be consistent with an e^+/μ^+ recoiling against the remaining tracks. We calculate the thrust axis [18] using all the charged and neutral deposits in the event and define two hemispheres with respect to the plane normal to the thrust axis. The e^+/μ^+ and the other tracks are required to be in separate hemispheres.

The τ has a fixed CM energy and momentum:

$$\begin{aligned} E_\tau^* &= \frac{\sqrt{s}}{2} + \frac{(M_\tau^2 - M_l^2)}{2\sqrt{s}} \\ \mathbf{p}_\tau^* &= \sqrt{E_\tau^{*2} - M_\tau^2} \end{aligned} \quad (1)$$

where M_τ and M_l are the masses of the τ and e^+/μ^+ , respectively [4]. We define the direction of the τ as opposite to that of the e^+/μ^+ and assign it the momentum from Equation 1. The CM four-momentum of the missing neutrino from the τ decay, p_ν^* , is defined as $p_\nu^* = p_\tau^* - p_\pi^*$, where p_π^* is the sum of the CM four-momenta of the pions. The reconstructed m_τ mass is defined to be $m_\tau = \sqrt{(E_\pi^* + |\mathbf{p}_\nu^*|)^2 - |\mathbf{p}_\tau^*|^2}$ where E_π^* is the CM energy of the pions.

The signal-background separation is mainly performed by considering ΔE , the difference between the e^+/μ^+ CM energy and $\sqrt{s}/2$, $\Delta E = E_l^* - \sqrt{s}/2$. Events are rejected if ΔE is less than -0.5 GeV or greater than 0.2 GeV. True signal events will have $\Delta E \sim -0.15$ GeV while $e^+e^- \rightarrow \mu^+\mu^-$ or $e^+e^- \rightarrow e^+e^-$ events will peak at zero and $e^+e^- \rightarrow \tau^+\tau^-$ background events have large negative ΔE . The ΔE resolution is approximately 50 MeV.

3.1. Optimization of the Signal Selection

We use a number of kinematic variables to further suppress backgrounds. The missing event energy in the CM frame, E_{miss}^* , is defined as the difference between \sqrt{s} and the sum of the charged track energies. It is distributed uniformly for signal but peaks at zero or near $\sqrt{s}/2$ for the

most important backgrounds. The missing mass squared, m_{miss}^2 , should be consistent with zero. A requirement on the maximum neutral energy cluster in the detector, E_γ , eliminates events with neutral pions or photons [19]. A requirement on the angle between the direction of the neutrino and the beam axis in the CM system, $\cos^*(\theta_\nu)$, ensures that the reconstructed neutrino direction is within the detector acceptance to reject events with significant radiation along the beam direction. The angle in the CM system between the direction of the neutrino and the τ , $\theta_{\tau\nu}^*$, is used to reject background events with a back-to-back track topology such as dimuon and Bhabha production. An event is accepted if it falls within a two-dimensional region defined with respect to m_τ and the e^+/μ^+ CM momentum, p_l^* . Events in this region are then used in a maximum likelihood fit to extract the signal yield.

Table 1
Selection criteria. Unless stated otherwise, identical criteria are used for both lepton flavors.

$\tau \rightarrow$	$\pi^-\pi^+\pi^-\nu_\tau$	$\pi^-\nu_\tau$
$E_{\text{miss}}^*(\mu\tau)$ (GeV)	0.015 – 3.23	0.65 – 4.55
$E_{\text{miss}}^*(e\tau)$ (GeV)	0.015 – 3.23	0.65 – 4.00
m_{miss}^2 (GeV^2/c^4)	< 0.56	< 0.65
E_γ (GeV)	< 0.20	< 0.15
$\cos^*(\theta_\nu)$	–0.9 – 0.9	–0.9 – 0.7
$\theta_{\tau\nu}^*$	> 0.015	> 0.09
m_τ (GeV/c^2)	1.6 – 2.0	1.6 – 2.0
p_l^* (GeV/c)	4.90 – 5.32	5.02 – 5.32
$\varepsilon_{\text{sig}}^{MC}(\mu\tau)$ (%)	18.5 ± 0.2	9.62 ± 0.14
$\varepsilon_{\text{sig}}^{MC}(e\tau)$ (%)	11.7 ± 0.2	11.9 ± 0.2

The values of the selection criteria are shown in Table 1. We optimize the selection sensitivity by defining a nominal signal box with a width of three standard deviations in the reconstructed m_τ and p_l^* . The resolutions on m_τ and p_l^* are approximately $10 \text{ MeV}/c^2$ and $45 \text{ MeV}/c$, respectively. The values of the selection criteria are cho-

sen to maximize the discriminant S/\sqrt{B} where S is the number of MC signal events in the nominal signal box and B is the number of data events accepted outside this region but within $1.5 < m_\tau < 2.2 \text{ GeV}/c^2$ and the p_l^* boundaries given in Table 1. As a cross-check, the procedure was repeated using background MC within the nominal signal box instead of data and this produced consistent results. The signal MC reconstruction efficiencies and their statistical uncertainties after the application of these selection criteria are also shown in Table 1.

The backgrounds are dominated by $e^+e^- \rightarrow \tau^+\tau^-$ decays where one τ decays to an e^+/μ^+ plus neutrinos and the other to either $\pi^-\pi^+\pi^-\nu_\tau$ or $\pi^-\nu_\tau$. Light quark continuum processes are predicted to contribute significantly to $e^+e^- \rightarrow \mu^+\tau^-(\tau^- \rightarrow \pi^-\pi^+\pi^-\nu_\tau)$ only and events from $e^+e^- \rightarrow \mu^+\mu^-$ are only present in $e^+e^- \rightarrow \mu^+\tau^-(\tau^- \rightarrow \pi^-\nu_\tau)$. Charm and $B\bar{B}$ backgrounds are eliminated by the track multiplicity and ΔE requirements and all other backgrounds are negligible. As a validation check, we compare the predicted MC background levels and distributions of the variables from Table 1 to the data in the region outside the nominal signal box and find that they are in agreement.

4. SIGNAL YIELD EXTRACTION

An extended unbinned maximum likelihood (ML) fit to the variables m_τ and p_l^* is used to extract the total number of signal and background events separately for each mode. The likelihood function is:

$$\mathcal{L} = \frac{e^{-\sum_j n_j}}{N!} \prod_i \sum_j n_j \mathcal{P}_j(\vec{x}_i) \quad (2)$$

where n_j is the yield of events of hypothesis j (signal or background) and N is the number of events in the sample. The individual background components comprise $e^+e^- \rightarrow \tau^+\tau^-$, $e^+e^- \rightarrow \mu^+\mu^- (\gamma)$ and light quark continuum decay modes. $\mathcal{P}_j(\vec{x}_i)$ is the corresponding probability density function (PDF), evaluated with the variables $\vec{x}_i = \{m_\tau, p_l^*\}$ for the i th event. For the signal, we use double Crystal Ball functions [20]

for both m_τ and p_l^* . Due to correlations between m_τ and p_l^* for non-signal events, we use a two-dimensional non-parametric PDF obtained from MC [21] for the backgrounds. In the maximum likelihood fit to the data, the parameters of the PDFs are fixed to the values determined from MC and only the signal and the background component yields are allowed to float.

We test the fitting procedure before unblinding the yields by fitting the data with the background PDFs only and allowing the yields of the MC background components to float. A varying number of signal MC events are then embedded in the background distributions and the full fit performed a number of times. The distribution of fitted signal yields is centered on the number of embedded signal events, showing that the fits are unbiased. We also perform fits where the relative yields of the MC background components are changed and confirm that changes in the ratio of the individual background MC components do not bias the fitted signal yield.

As a validation check, we extrapolate the fitted background PDFs from the region outside the nominal signal region into the nominal signal region. We predict 193 ± 9 and 112 ± 7 events for the 3-prong τ decay $e^+e^- \rightarrow \mu^+\tau^-$ and $e^+e^- \rightarrow e^+\tau^-$ channels. For the 1-prong τ decay $e^+e^- \rightarrow \mu^+\tau^-$ and $e^+e^- \rightarrow e^+\tau^-$ reactions, we obtain 143 ± 7 and 90 ± 6 events respectively. All uncertainties are statistical only, and the number of data events in the same region is 202, 128, 154 and 75 respectively.

From the reconstructed MC efficiency, we can estimate the expected number of background events and compare to the result of the ML fit. For $e^+e^- \rightarrow \tau^+\tau^-$, the predicted background in the fitted region is 750 ± 43 and 414 ± 41 events for the 3-prong τ decay $e^+e^- \rightarrow \mu^+\tau^-$ and $e^+e^- \rightarrow e^+\tau^-$ channels. The MC prediction for the 1-prong τ decay $e^+e^- \rightarrow \mu^+\tau^-$ and $e^+e^- \rightarrow e^+\tau^-$ channels is 494 ± 40 and 319 ± 45 events. The ML fit returns 775 ± 19 , 518 ± 41 , 385 ± 35 and 331 ± 18 events respectively. The dimuon background to $e^+e^- \rightarrow \mu^+\tau^-(\tau^- \rightarrow \pi^-\nu_\tau)$ is predicted to be 114 ± 38 events from MC and is measured to be 189 ± 30 . The light continuum cross section is not well known but the MC predicts 119 ± 24 and $19 \pm$

9 events for $e^+e^- \rightarrow \mu^+\tau^-(\tau^- \rightarrow \pi^-\pi^+\pi^-\nu_\tau)$ and $e^+e^- \rightarrow e^+\tau^-(\tau^- \rightarrow \pi^-\pi^+\pi^-\nu_\tau)$ respectively, with 129 ± 40 and 18 ± 35 measured by the ML fit.

The main sources of systematic uncertainties come from uncertainties in the reconstruction, the $\tau^- \rightarrow \pi^-\pi^+\pi^-\nu_\tau$ decay mechanism and the fit procedure. A relative systematic uncertainty of 0.8% is applied for the reconstruction efficiency added linearly for each charged track. A relative systematic uncertainty of 1.0% added linearly for each charged pion track and 1.3% for each e^+/μ^+ is applied to account for differences in MC and data particle identification efficiencies.

A possible non-axial-vector decay mechanism for the decay $\tau^- \rightarrow \pi^-\pi^+\pi^-\nu_\tau$ is not completely ruled out by current measurements [4]. To estimate this effect, the signal MC events are generated with 90% axial-vector and 10% phase-space decays and the difference in the reconstruction efficiency compared to 100% a_1^- (1260) decays applied as a systematic. This introduces a relative systematic uncertainty of 3.2%.

The largest systematic uncertainties come from the variation of the PDF fit parameters within their fitted uncertainties and from varying the selection criteria by their expected resolution. The two-dimensional non-parametric background PDFs show small structures that depend on MC statistics and the value of the smoothing parameter [21] used. By varying the smoothing parameter, using different functional forms and varying the fitted parameters within their uncertainties, we derive a systematic uncertainties of ~ 0.5 events. Repeating the analysis with the selection cuts varied by the resolution on the selection variables introduces an uncertainty of 2.5 to 4.4 events associated with scale and resolution uncertainties of these variables and a small contribution from the beam energy uncertainty. The total systematic uncertainty is between 2.6 and 4.4 events and our final limit on the cross sections is dominated by the statistical error which is of the order of 10 events.

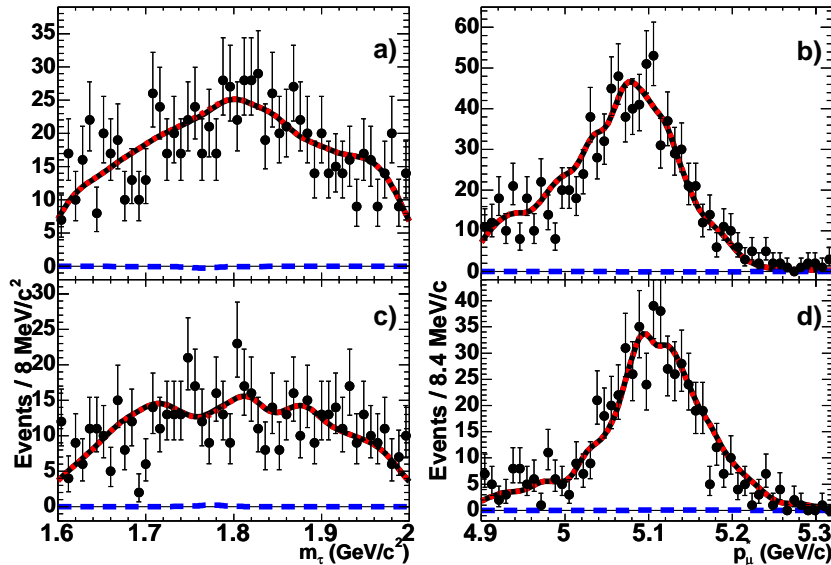


Figure 1. Reconstructed distributions of the fit variables for $e^+e^- \rightarrow \mu^+\tau^-$ candidates: a) m_τ and b) p_μ^* for $\tau^- \rightarrow \pi^-\pi^+\pi^-\nu_\tau$; and c) m_τ and d) p_μ^* for $\tau^- \rightarrow \pi^-\nu_\tau$. The projection of the ML fit (solid black line) hides the background component (dotted red line). The projection of the few signal events is shown on the horizontal axis as a dashed blue line.

5. RESULTS

The m_τ and p_μ^* distributions for the modes are shown in Figures 1 and 2. The projection of the signal PDF is shown as the dashed blue line, the background PDFs as the dotted red line and the total PDF as the solid black line. The central value of the cross section for $e^+e^- \rightarrow l^+\tau^-$ is given by $\sigma = N/\eta\epsilon\mathcal{L}$ where N is the number of signal events, η the signal reconstruction efficiency and ϵ is the $\tau^- \rightarrow \pi^-\pi^+\pi^-\nu_\tau$ or $\tau^- \rightarrow \pi^-\nu_\tau$ branching fraction. The measurements are not statistically different from the null hypothesis and we obtain 95% CL upper limits by finding the maximum number of signal events N such that the integral of the total likelihood function is 95% of the total integral. From MC studies [13], the total cross section of the process $e^+e^- \rightarrow \mu^+\mu^-$ at $\sqrt{s} = 10.58$ GeV is $\sigma_{\mu\mu} = (1.13 \pm 0.02)$ nb and we use this to calculate 95% CL upper limits on the ratio of the cross sections with respect to the

dimuon cross section. The central values of the signal yields from the maximum likelihood fit and the upper limits on the cross sections and cross section ratios are given in Table 2.

We combine the $\tau^- \rightarrow \pi^-\pi^+\pi^-\nu_\tau$ and $\tau^- \rightarrow \pi^-\nu_\tau$ decays and calculate 95% CL upper limits on the cross sections of < 4.6 fb for $e^+e^- \rightarrow \mu^+\tau^-$ and < 10.1 fb for $e^+e^- \rightarrow e^+\tau^-$. The 95% CL upper limits on the ratios of the cross sections with respect to the dimuon cross section are calculated to be $\sigma_{\mu\tau}/\sigma_{\mu\mu} < 4.0 \times 10^{-6}$ and $\sigma_{e\tau}/\sigma_{\mu\mu} < 8.9 \times 10^{-6}$.

In conclusion, we have performed the first search at a CM energy of $\sqrt{s} = 10.58$ GeV of the lepton-flavor-violating production processes $e^+e^- \rightarrow \mu^+\tau^-$ and $e^+e^- \rightarrow e^+\tau^-$ using the BABAR detector. No statistically significant signal events were observed in any of the decay modes. 95% CL upper limits have been placed on the cross sections and ratios of cross sections to the dimuon cross section to form the most strin-

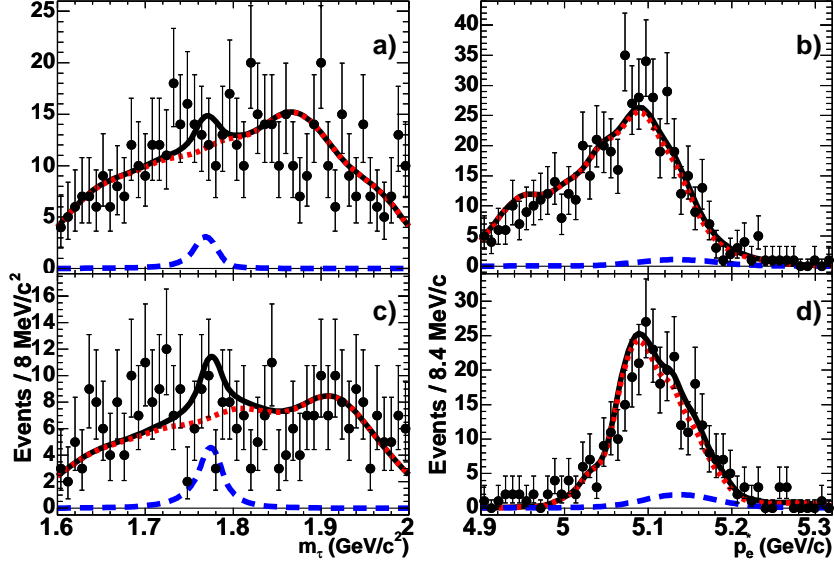


Figure 2. Reconstructed distributions of the fit variables for $e^+e^- \rightarrow e^+\tau^-$ candidates: a) m_τ and b) p_e^* for $\tau^- \rightarrow \pi^-\pi^+\pi^-\nu_\tau$; and c) m_τ and d) p_e^* for $\tau^- \rightarrow \pi^-\nu_\tau$. The solid black line is the projection of the ML fit and the dotted red line is the background component. The projection of the signal events is shown on the horizontal axis as a dashed blue line.

Table 2

Results for the signal yields, cross sections and ratios of cross sections to the dimuon cross section. The first uncertainty is statistical and the second systematic.

	$e^+e^- \rightarrow \mu^+\tau^-$		$e^+e^- \rightarrow e^+\tau^-$	
	$\tau^- \rightarrow \pi^-\pi^+\pi^-\nu_\tau$	$\tau^- \rightarrow \pi^-\nu_\tau$	$\tau^- \rightarrow \pi^-\pi^+\pi^-\nu_\tau$	$\tau^- \rightarrow \pi^-\nu_\tau$
Total Events	905	575	537	332
Signal Events	$-1.4 \pm 9.9 \pm 2.6$	$1.9 \pm 10.1 \pm 4.4$	$15.9 \pm 10.3 \pm 2.7$	$10.7 \pm 8.8 \pm 2.7$
$\sigma_{l\tau}$ (fb)	$-0.4 \pm 2.6 \pm 0.7$	$0.9 \pm 4.5 \pm 2.0$	$6.5 \pm 4.2 \pm 1.1$	$3.9 \pm 3.2 \pm 1.0$
$\sigma_{l\tau}$ (95% CL) (fb)	< 5.9	< 11.4	< 14.8	< 11.1
$\sigma_{l\tau}/\sigma_{\mu\mu}$ (95% CL)	$< 5.2 \times 10^{-6}$	$< 10.1 \times 10^{-6}$	$< 13.1 \times 10^{-6}$	$< 9.8 \times 10^{-6}$

gent limits on $e^+e^- \rightarrow \mu^+\tau^-$ and $e^+e^- \rightarrow e^+\tau^-$ measured so far.

REFERENCES

1. B. T. Cleveland *et al.*, Homestake Collaboration, *Astrophys. J.* 496, 505 (1998); Super-Kamiokande Collaboration, Y. Fukuda *et al.*, *Phys. Rev. Lett.* 81, 1562 (1998); Q. R. Ahmad *et al.*, SNO Collaboration, *Phys. Rev. Lett.* 89, 011301 (2002).
2. E. Ma, *Nucl. Phys. Proc. Suppl.* 123, 125 (2003).
3. B. W. Lee, R. E. Shrock, *Phys. Rev. D* 16, 1444 (1977).

4. Particle Data Group, S. Eidelman *et al.*, J. Phys. G33, 1 (2006).
5. B. Aubert *et al.*, BABAR Collaboration, Phys. Rev. Lett. 95, 041802 (2005); Phys. Rev. Lett. 96, 041801 (2006).
6. J. Bordes, H.-M. Chan, S. T. Tsou, hep-ph/0111175; Phys. Rev. D 65, 093006 (2002); Eur. Phys. Jour. C 27, 189 (2003).
7. J. J. Gomez-Cadenas *et al.*, MARK II Collaboration, Phys. Rev. Lett. 66, 1007 (1991).
8. R. Akers *et al.*, OPAL Collaboration, Z. Phys. C 67, 555 (1995); P. Abreu *et al.*, DELPHI Collaboration, Z. Phys. C 73, 243 (1996).
9. G. Abbiendi *et al.*, OPAL Collaboration, Phys. Lett. B 519, 23 (2001); LEP Collaborations, CERN-PH-EP-2005-051 (2005).
10. B. Aubert *et al.*, BABAR Collaboration, Nucl. Instr. Meth. A 479, 1 (2002).
11. D. J. Lange, Nucl. Instr. Meth. A 462, 152 (2001).
12. E. Barberio, Z. Was, Comput. Phys. Commun. 79, 291 (2004).
13. S. Jadach, Z. Was, Comput. Phys. Commun. 85, 453 (1995).
14. S. Jadach, Z. Was, R. Decker, J. H. Kuhn, Comput. Phys. Commun. 76, 361 (1993).
15. R. A. Briere *et al.*, CLEO Collaboration, Phys. Rev. Lett. 90, 181802 (2003).
16. B. F. Ward, S. Jadach, Z. Was, Nucl. Phys. Proc. Suppl. 116, 73 (2003); T. Sjöstrand, Comput. Phys. Commun. 82, 74 (1994);
17. S. Agostinelli *et al.*, GEANT4 Collaboration, Nucl. Instr. Meth. A 506, 250 (2003).
18. S. Brandt *et al.*, Phys. Lett. B 12, 57 (1964); E. Fahri, Phys. Rev. Lett. 39, 1587 (1977).
19. B. Aubert *et al.*, BABAR Collaboration, Phys. Rev. D 73, 057101 (2006).
20. T. Skwarnicki, Ph.D. thesis, Cracow Institute of Nuclear Physics, DESY-F31-86-02, 1986.
21. K. Cranmer, Comput. Phys. Commun. 136, 198 (2001).